

# Synthesis and Selective Recognition Toward Zinc Ion of Chiral Poly(Imine-Triazole)

Jinting Zhou, Wei Lu, Fangyu Hu, Mengyu Zhang, Liming Jiang, Zhiquan Shen

MOE Key Laboratory of Macromolecular Synthesis and Functionalization, Department of Polymer Science and Engineering, Zhejiang University, Hangzhou 310027, China

Correspondence to: L. Jiang (E-mail: cejlm@zju.edu.cn)

Received 3 December 2013; accepted 12 April 2014; published online 10 May 2014

DOI: 10.1002/pola.27223

**ABSTRACT:** A novel AB type of clickable monomer, (S)-2-[(2-azido-1-phenylethylimino)methyl]-5-propargyloxyphenol (AMPP) was designed and polymerized to yield a class of main-chain chiral poly(imine-triazole)s through the metal-free click reaction. With the thermally induced polymerization, the desired polytriazoles can be easily prepared in high yields by a stepwise heating-up process and have the number-average molecular masses ranging from  $5.1 \times 10^3$  to  $58.1 \times 10^3$  (polydispersity indices = 1.38–1.68). The polymers were characterized by Fourier Transform Infrared spectroscopy (FTIR),  $^1\text{H}$  Nuclear Magnetic Resonance (NMR), and gel permeation chromatography, and their optical properties were studied by fluorescence and circular dichroism (CD) spectroscopies. As a chemosensor, these polymers exhibited a selective “turn-on” fluorescence enhance-

ment response toward  $\text{Zn}^{2+}$  ion over other cations such as  $\text{Na}^+$ ,  $\text{K}^+$ ,  $\text{Mg}^{2+}$ ,  $\text{Ca}^{2+}$ ,  $\text{Ag}^+$ ,  $\text{Pb}^{2+}$ ,  $\text{Cd}^{2+}$ ,  $\text{Hg}^{2+}$ ,  $\text{Mn}^{2+}$ , and  $\text{Ni}^{2+}$  in dimethyl sulfoxide. However, the  $\text{Zn}^{2+}$ -induced fluorescence signal was subject to serious interference by  $\text{Al}^{3+}$ ,  $\text{Cu}^{2+}$ ,  $\text{Cr}^{3+}$ , and  $\text{Fe}^{3+}$  ions. Interestingly, the chiral polymer showed distinctive changes in the CD spectra on complexation with  $\text{Zn}^{2+}$ , which allowed for the discrimination of this ion in the presence of other species tested including those interfering ions observed in the fluorescent detection. © 2014 Wiley Periodicals, Inc. *J. Polym. Sci., Part A: Polym. Chem.* **2014**, *52*, 2248–2257

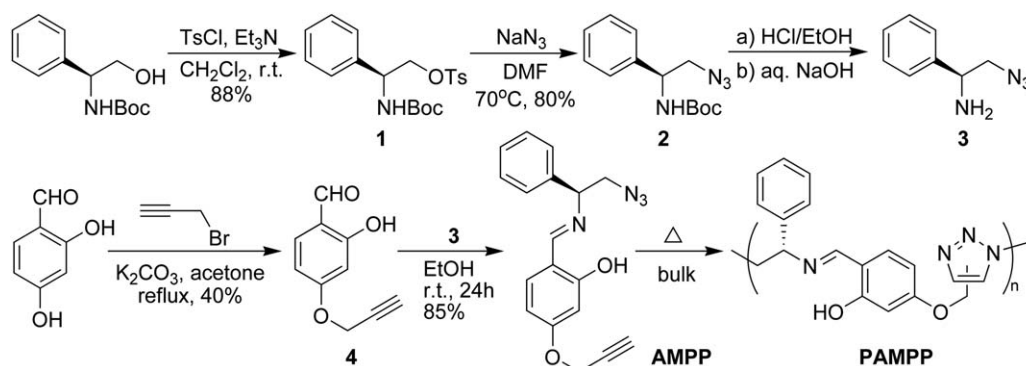
**KEYWORDS:** click reaction; chiral; fluorescence; polytriazole; sensors; zinc ion

**INTRODUCTION** Click chemistry encompasses a class of reactions that allow the coupling of two molecular fragments in an extremely effective manner.<sup>1,2</sup> The most widely utilized of these efficient transformation reactions is the copper(I)-catalyzed 1,3-dipolar cycloaddition of azides and alkynes, which results in the formation of 1,4-disubstituted 1,2,3-triazoles in high yields and with excellent regioselectivity.<sup>3</sup> In the last 10 years, this simple click reaction has been creatively used to facilitate the synthesis of complex-structured polymers and modification of material surfaces.<sup>4</sup> In the meantime, the properties of the functional 1,2,3-triazole motif have also begun to attract a lot of research interest. The numerous studies on supramolecular systems involving macrocyclic triazolophanes and oligotriazoles demonstrated that the triazole unit exhibits the ability to simultaneously play the role of hydrogen-bond acceptor and hydrogen-bond donor; that is, the lone pair on the middle nitrogen atom can act as a hydrogen-bond acceptor, whereas the polarized C–H bond takes the role of a nonclassical hydrogen-bond donor.<sup>5</sup> These marvellous features of triazole ring make it an ideal building block not only in supramolecular chemistry but also for the construction of polymeric materials for optoelectronic, biomedical, and pharmaceu-

tical applications.<sup>6</sup> Nevertheless, there are fairly limited reports on polymeric sensors incorporating the triazole moiety. Lately, Yashima and coworkers<sup>7</sup> developed a facile method to prepare optically active helical poly(phenylacetylene)s via the click polymer reaction of optically inactive azide-bound poly(phenylacetylene)s with chiral acetylenes. The resulting polymers formed a preferred-handed helical conformation and exhibited characteristic induced circular dichroisms (CDs) whose Cotton effect (CE) signs can be used to sense the chirality of the chiral acetylenes. The Cheng group synthesized several conjugated polymers containing triazole units in the main chain by using Cu(I) catalyzed azide–alkyne cycloaddition.<sup>8</sup> As fluorescence sensors these polytriazoles showed a pronounced fluorescence response for  $\text{Ni}^{2+}$  or  $\text{Hg}^{2+}$  with excellent selectivity over other transition metal ions, such as  $\text{Cu}^{2+}$ ,  $\text{Zn}^{2+}$ ,  $\text{Co}^{2+}$ , and  $\text{Cd}^{2+}$ . More recently, Qin and coworkers reported tetraphenylethene-containing polytriazoles prepared through the metal-free click polymerization.<sup>9</sup> They found that the polymers exhibit the aggregation-induced emission characteristics and the aggregates formed in tetrahydrofuran (THF)/water mixture can serve as a fluorescent probe for detecting explosives such as picric acid.

Additional Supporting Information may be found in the online version of this article.

© 2014 Wiley Periodicals, Inc.



**SCHEME 1** Synthesis of the functional monomer AMPP and its click polymerization.

Over the course of our research on artificial chemosensors for ions of biological importance, we developed an effective method for  $\text{Zn}^{2+}$  detection using a structurally simple Schiff base derivative as a sensor.<sup>10</sup> The probe molecule displayed high affinity for zinc ion over other cations of interest including  $\text{Cd}^{2+}$  in unbuffered methanol. In general, compared to the chemosensors based on small organic molecules, polymeric counterparts would offer some advantages such as signal amplification, enhanced binding efficiency and selectivity for a specific analyte by virtue of the possible cooperative effects of multiple recognition sites.<sup>11</sup> In this aspect, we are particularly interested in exploring chiral polymer-based fluorescent sensors, because such sensory systems would provide a chiroptical signal that indicates guest binding.<sup>12</sup> As a part of our continuing efforts in the field, this article deals with the synthesis and structural characterization of a new kind of main-chain chiral poly(imine-triazole)s as well as the investigation of its luminescent and chiroptical properties on exposure to targeted metal ions. The results revealed that the polymer sensor exhibited differing spectral changes on binding with  $\text{Zn}^{2+}$ , which can be used to effectively distinguish this ion from the common metal ions. To the best of our knowledge, there are very few currently reported applications of chiral polymers in cation detection; especially, main-chain chiral polytriazole-based sensors for selective  $\text{Zn}^{2+}$  recognition have scarcely been described so far.

## EXPERIMENTAL

### Materials

Boc-(*S*)-phenylglycinol, sodium azide, 1-hexyne, triethylamine, and *N,N,N',N''*-pentamethyldiethylenetriamine (PMDETA, 98%) were purchased from Sigma-Aldrich and used as received without further purification. Dichloromethane ( $\text{CH}_2\text{Cl}_2$ ), *N,N*-dimethylformamide (DMF), dimethyl sulfoxide (DMSO), and other organic solvents were commercially available (Sinopharm Chemical Reagent) and purified by standard methods prior to use.

### Measurements

$^1\text{H}$  and  $^{13}\text{C}$  NMR spectra were recorded on a BrukerAvance AMX-400 and 500 NMR spectrometer, respectively. A Bruker Vector 22 Fourier Transform Infrared spectrophotometer was

applied for recording infrared spectroscopy (IR) spectra in KBr pellets. Electrospray ionization mass spectrometry (ESIMS) was measured on a Bruker Esquire<sup>3000</sup> plus ion trap mass spectrometer. The polymer molecular weights ( $M_w$ ,  $M_n$ ) and polydispersity ( $M_w/M_n$ ) were measured on a Waters-150C gel permeation chromatography system. Monodisperse poly(methyl methacrylate) was used as calibration standards and DMF as the eluent at a flow rate of 1.0 mL  $\text{min}^{-1}$  at 60 °C. Steady-state fluorescence spectra were measured on a PerkinElmer LS-55 fluorescence spectrometer in the right-angle geometry (90° collecting optics). UV-vis and CD spectra were obtained in DMSO at 25 °C using a quartz cell of 1 cm on MOS-450 (Biologic Company, France).

### Synthesis of Monomer AMPP

To a solution of Boc-(*S*)-phenylglycinol (1.25 g, 5.2 mmol) in 20 mL anhydrous  $\text{CH}_2\text{Cl}_2$  were added  $\text{Et}_3\text{N}$  (1.45 mL, 10.4 mmol) and *p*-toluenesulfonyl chloride (1.25 g, 5.2 mmol; Scheme 1). The reaction mixture was allowed to stir at room temperature under  $\text{N}_2$  atmosphere for 24 h, and was then quenched with aqueous 10%  $\text{K}_2\text{CO}_3$  solution (20 mL). After stirring for 2 h, the aqueous layer was separated and extracted with  $\text{CH}_2\text{Cl}_2$  ( $2 \times 30$  mL). The combined organic extracts were washed with deionized water, dried over anhydrous  $\text{MgSO}_4$ , filtered, and evaporated under reduced pressure to give a solid residue. The crude product was recrystallized in EtOAc/*n*-hexane (1:2) to afford **1** as a white solid (yield 88%).

A mixture of **1** (0.5 g, 1.5 mmol) and  $\text{NaN}_3$  (0.13 g, 2 mmol) in anhydrous DMF (10 mL) was stirred at 70 °C under  $\text{N}_2$  atmosphere. After 24 h, the reaction mixture was poured into deionized water (50 mL); the collected precipitate was then recrystallized in DMF/water (1:5) give **2** as a white powder (yield 80%).

To a stirred solution of **2** (0.84 g, 4 mmol) in EtOAc (3 mL) was added dropwise 6 mL 2.5 M HCl/EtOAc at 0 °C. After stirring for 6 h from 0 °C to room temperature, the reaction mixture was concentrated via rotary evaporator and stirred with 5 M NaOH aqueous solution (100 mL) for another 6 h, and then extracted with  $\text{CH}_2\text{Cl}_2$  ( $2 \times 30$  mL). The organic extract was washed with deionized water, dried (anhydrous

MgSO<sub>4</sub>), filtered, and evaporated under reduced pressure to give **3** as a pale-yellow oil in near 100% yield.

Under N<sub>2</sub> atmosphere and magnetic stirring, propargyl bromide (0.6 g, 5 mmol) was added into the flask containing 2,4-dihydroxybenzaldehyde (0.7 g, 5 mmol) and K<sub>2</sub>CO<sub>3</sub> (0.7 g) in anhydrous acetone (20 mL). The reaction mixture was refluxed for 6 h. After filtration, the organic layer was washed with deionized water, dried (MgSO<sub>4</sub>), and evaporated under reduced pressure to yield a solid residue. The crude product was purified by flash column chromatography (CH<sub>2</sub>Cl<sub>2</sub>/*n*-hexane, 1/1) to afford **4** as white needle crystals (yield 40%).

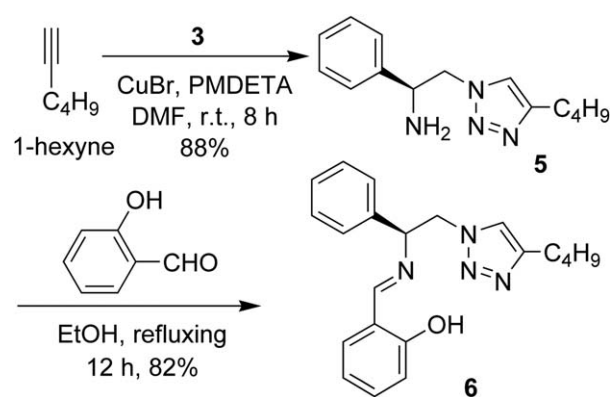
**3** (0.72 g, 4 mmol) and **4** (0.8 g, 4 mmol) were dissolved in 10-mL ethanol and then the reaction mixture was allowed to stir at room temperature for 24 h. After removing the solvent via rotary evaporator, the resulted residue was recrystallized with ethanol to give the desired product (*S*)-2-[(2-azido-1-phenylethylimino)methyl]-5-propargyloxyphenol (AMPP) as yellow crystals (1.3 g, yield 85%). M.p. 59.0–59.2 °C;  $[\alpha]_D^{20} = -74.4^\circ$  (*c* 0.5, DMSO); <sup>1</sup>H NMR (DMSO-*d*<sub>6</sub>, 400 MHz): δ 13.55 (s, 1H), 8.63 (s, 1H), 7.56–7.23 (m, 4H), 6.57–6.36 (m, 2H), 4.84 (2H, *J* = 2.3 Hz), 4.66 (dd, 1H, *J* = 8.6 Hz), 3.83 (1H, dd, *J* = 8.6 Hz), 3.71 (dd, 1H, *J* = 8.5 Hz), 3.61 (s, 1H, *J* = 2.3 Hz); <sup>13</sup>C NMR (DMSO-*d*<sub>6</sub>, 125 MHz): δ 166.6, 163.2, 161.5, 140.5, 133.8, 129.2, 128.3, 127.5, 113.3, 107.3, 102.3, 79.3, 79.0, 71.7, 56.5, 56.1; FTIR (KBr, cm<sup>-1</sup>): 3442, 3292, 2929, 2104, 1630, 1298, 1144, 822. MS [ESI, *m/z* ([*M*+*H*)<sup>+</sup>]: Calculated 321.1, Found 321.1.

### Preparation of Poly(Imine-Triazole)s by Bulk Polymerization

Typically, 0.1 g of AMPP was placed in a 10 mL ampoule and degassed by being subjected to the freeze-thaw cycle three times. Then, the ampoule was sealed under vacuum and immersed in a constant-temperature oil bath. After being heated for a definite period of time, the reaction was terminated by putting the ampoules into liquid nitrogen. The crude product was dissolved in DMF and precipitated from methanol. Further purification could be conducted by repeating this process twice. The resulting polymer (PAMPP) was dried to a constant weight in vacuum at 40 °C. The same method was used for the solution polymerizations in DMF.

### Synthesis of Model Compound **6**

A mixture of **3** (0.2 g, 1.2 mmol), 1-hexyne (0.1 g, 1.2 mmol), CuBr (0.09 g, 0.6 mmol), and PMDETA (0.107 g, 0.6 mmol) in 15 mL DMF was stirred at ambient temperature under N<sub>2</sub> atmosphere (Scheme 2). After stirring for 8 h, the solution was passed through neutral alumina to remove the copper catalyst. The elute was concentrated, and the residue was recrystallized in ethyl acetate/*n*-hexane (1:1) to give **5** as a white solid (0.26 g). Then, the intermediate was dissolved in 20 mL of ethanol together with 0.13 g of salicylaldehyde. The reaction mixture was refluxed for 12 h, and the solvent was removed under vacuum. The resulting residue was recrystallized in ethanol to afford **6** as a pale yellow solid in a total yield of 72% (0.32 g). M.p. 99.5–100.5 °C;



**SCHEME 2** Synthetic route to the model compound **6**.

$[\alpha]_D^{20} = 41.8^\circ$  (*c* 0.5, DMSO); <sup>1</sup>H NMR (CDCl<sub>3</sub>, 400 MHz): δ 12.94 (s, 1H), 8.07 (s, 1H), 7.44–7.30 (m, 6H), 7.11 (d, 1H), 7.07 (s, 1H), 6.97 (d, 1H), 6.85 (t, 1H), 4.86 (m, 2H), 4.58 (m, 1H), 2.58 (m, 2H), 1.43 (m, 2H), 1.16 (m, 2H), 0.78 (m, 3H). FTIR (KBr, cm<sup>-1</sup>): 3435, 2927, 1630, 1277, 1061, 758.

### General Procedure for Metal Ion Recognition

Metal ion titration experiments were performed with a 2.0 mL DMSO solution of the polymer by adding aliquots of a solution of the selected salt at room temperature. Mercury perchlorate salt and other various metal nitrate salts (aqueous solution of 1.0 × 10<sup>-2</sup> mol L<sup>-1</sup>) were used in the titration. The polymer concentration (based on monomeric units) was 1.0 × 10<sup>-4</sup> mol L<sup>-1</sup> for UV-vis and CD measurements and 1.0 × 10<sup>-5</sup> mol L<sup>-1</sup> for fluorescence detection. Before each measurement, the sample solution containing the polymer and metal ions with different molar ratios was allowed to stand at ambient temperature for 2 h with the view of insuring complete host-guest complexation.

## RESULTS AND DISCUSSION

### Monomer Synthesis and Thermal 1,3-Dipolar Cycloaddition Reaction

The synthesis procedures for the monomer (*S*)-2-[(2-azido-1-phenylethylimino)methyl]-5-propargyloxyphenol (AMPP) and the corresponding polymer (PAMPP) are shown in Scheme 1. The monomer is a chiral Schiff base derivative of salicylaldehyde containing alkyne and azide groups, which was readily prepared from commercially available starting materials by simple functional-group transformations. The well-defined chemical structure of AMPP was confirmed by various spectroscopic techniques, such as FTIR, NMR, and ESIMS (see Experimental part and Supporting Information Figs. S1–S4).

Knowing that the Cu<sup>I</sup>-catalyzed azide–alkyne cycloaddition has been developed as a powerful technique in polymer syntheses,<sup>4</sup> we first tried to use it to polymerize AMPP in DMF. The results showed that the monomer seemed to be considerably reactive and the expected polymerization occurred smoothly at 50 °C. However, the purification of the resultant products was very difficult so that we failed to get the

**TABLE 1** Results on the Metal-Free Click Polymerization of AMPP

Entry	Reaction conditions		Polymers					
	Temp. (°C)/Time (h)	[AMPP] (mol L <sup>-1</sup> ) <sup>a</sup>	Code	Yield (%)	<i>M</i> <sub>n</sub> <sup>b</sup> (10 <sup>3</sup> )	PDI <sup>b</sup>	<i>F</i> <sub>1,4</sub> <sup>c</sup> (%)	[α] <sub>D</sub> <sup>20</sup> <sup>d</sup>
1	80/12	Bulk	PAMPP-1	89	5.1	1.38	63.0	+7.2
2	80/24	Bulk	PAMPP-2	92	5.6	1.40	62.6	+8.3
3	80/36	Bulk	PAMPP-3	90	5.8	1.43	62.4	+10.8
4	80/12+100/12	Bulk	PAMPP-4	94	7.3	1.48	62.1	+8.7
5	80/12+120/12	Bulk	PAMPP-5	94	13.7	1.66	63.0	+21.2
6	80/12+120/6+150/6	Bulk	PAMPP-6	95	58.1	1.68	62.3	+25.1
7	150/6	Bulk	PAMPP-7	93	57.4	1.89	62.5	+24.2
8	80/12	2.0	PAMPP-8	45	4.3	1.27	62.6	+10.7
9	80/12+120/12	2.0	PAMPP-9	67	23.7	1.65	61.9	+17.6

<sup>a</sup> DMF was used as solvent;

<sup>b</sup> Taken from GPC in DMF solution and calibrated against standard polymethylmethacrylate, PDI = *M*<sub>w</sub>/*M*<sub>n</sub>;

<sup>c</sup> Fraction of 1,4-regioisomeric units determined by <sup>1</sup>H NMR;

<sup>d</sup> The optical rotation values were measured in DMSO (*c* = 0.5).

desired polymer samples for structural characterizations.<sup>13</sup> The reason is probably related to the formation of Cu(II)-containing polymer complexes due to the strong affinity of both imine and triazole units toward the metal residue. Thus, we turned our attention to the metal-free click approach for production of poly(imine-triazole)s, which might be a more desirable alternative for developing fluorescent sensors because the residual copper ions would serve as a fluorescence quencher.<sup>14</sup>

The thermally induced polyaddition of AMPP was exploited in both bulk and solution states. As listed in Table 1, the bulk polymerizations conducted at 80 °C showed high levels of monomer conversion (89–92%) and yielded the polymers with lower molar masses (*M*<sub>n</sub> = 5.1 × 10<sup>3</sup> – 5.8 × 10<sup>3</sup>, Entries 1–3). At this temperature extending the reaction time had only a small effect on the *M*<sub>n</sub> value of resulting polymers. However, when the temperature was increased in steps up until 150 °C, significantly higher molar mass could be realized by longer reaction time (Entries 4–6). If performing the polyaddition directly at 150 °C, the molar mass of the polymer is comparable to that of PAMPP-5 obtained in the gradual heating-up mode, but a relatively broad polydispersity (*M*<sub>w</sub>/*M*<sub>n</sub> = 1.89) is observed (Entries 6, 7). The reason for this is likely associated with the greatly increased viscosity of the bulk polymerization system. Indeed, in the case of rapid elevation of polymerization temperature to 150 °C, a rather viscous reaction medium occurred at the early stage of polymerization. The high viscosity may decrease the homogeneity of the reaction system and thereby enlarge the molecular weight distribution to a certain extent. Conversely, the polymerization can also proceed in DMF with a moderate yield, and similarly, higher reaction temperatures are beneficial to the enhancement of polymer molar masses (Entries 8 and 9). The poly(imine-triazole)s formed in all cases have lower polydispersity indices (PDIs) than the theoretical value (2.0) typical of a step growth polymerization process, which

seems to be fairly common in the click polymerizations.<sup>4f–h,8,9a,b</sup> These polymers are only soluble in organic solvents with rather high polarity, such as DMF and DMSO. The specific rotation ([α]<sub>D</sub><sup>20</sup>) obtained in DMSO (see Table 1) for the polymers always shows the opposite sign to the one for the corresponding monomer ([α]<sub>D</sub><sup>20</sup> = –74.4°, *c* = 5 mg mL<sup>-1</sup>, DMSO), and the [α]<sub>D</sub><sup>20</sup> value increases roughly with the increasing of *M*<sub>n</sub>.

### Structural Characterization

IR spectra of AMPP and the polymer samples with an intentionally low and high molar mass are given in Figure 1. The monomer shows the characteristic absorption band at 3291 cm<sup>-1</sup> due to ≡C–H stretching vibration, while the absorption of C≡C nearly merged with that of azide groups around 2104 cm<sup>-1</sup>. It can be seen that these absorption bands become much weaker for PAMPP-1 (*M*<sub>n</sub> = 5.1 × 10<sup>3</sup>), even

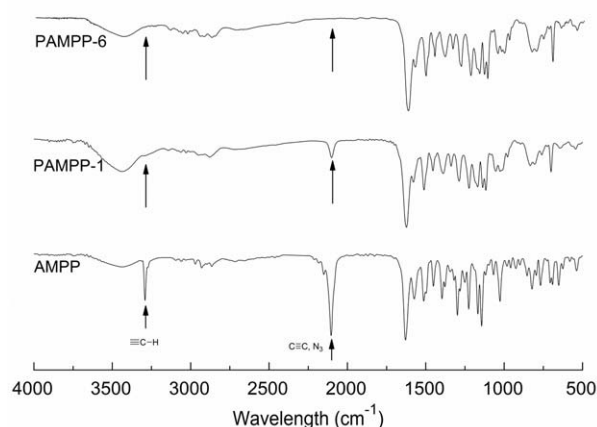


**FIGURE 1** Stacked FTIR spectra of AMPP and the polymers obtained under different reaction conditions. PAMPP-1 (*M*<sub>n</sub> = 5.1 × 10<sup>3</sup>), PAMPP-6 (*M*<sub>n</sub> = 58.1 × 10<sup>3</sup>), see: Table 1.

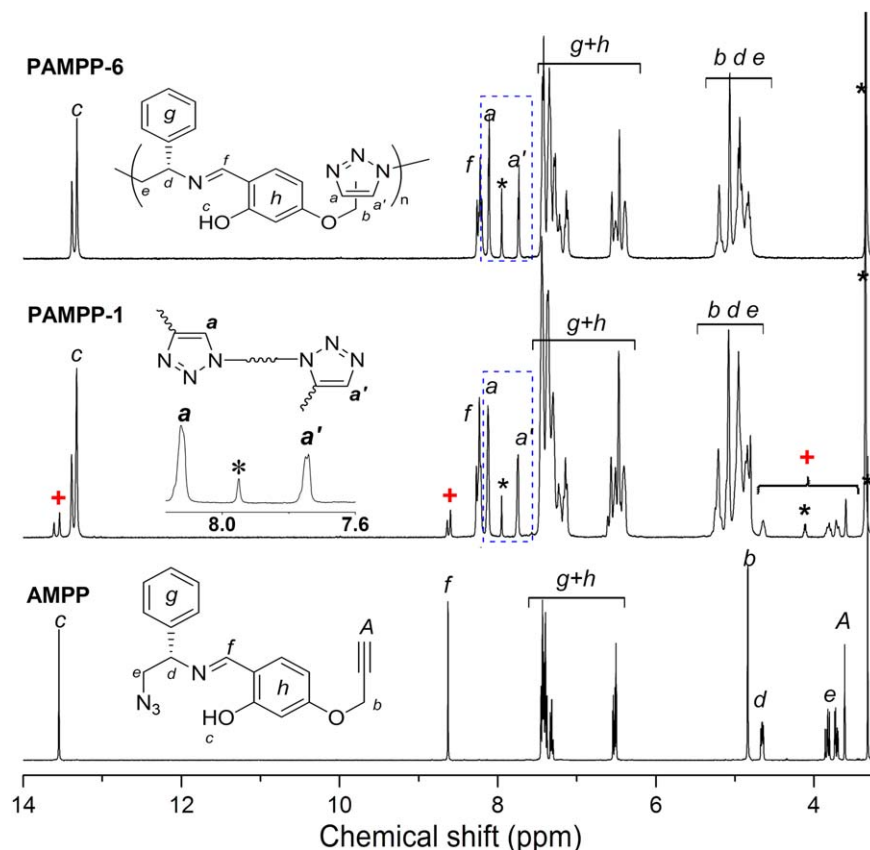


**FIGURE 2**  $^1\text{H}$  NMR spectra of AMPP and the corresponding polymers PAMPP-1 and PAMPP-6 in  $\text{DMSO-}d_6$ . The solvent peaks are marked with asterisks. [Color figure can be viewed in the online issue, which is available at [wileyonlinelibrary.com](http://wileyonlinelibrary.com).]

almost completely disappear for PAMPP-6 ( $M_n = 58.1 \times 10^3$ ). This indicates that the azide and alkyne groups of the monomers have been efficiently transformed into the triazole rings of the polymer by the metal-free promoted click reaction.

Figure 2 displays  $^1\text{H}$  NMR spectra of AMPP and the corresponding polymers PAMPP-1 and PAMPP-6. The signals due to alkyne group at 3.60 as well as those due to the methylene protons ( $e$ ) adjacent to the azido group of AMPP at 3.76 ppm decrease dramatically after polymerization, concomitant with appearance of the new peaks at  $\delta$  8.11 ( $a$ ) and 7.73 ( $a'$ ). Meanwhile, the azomethine proton signal ( $f$ ) in the polymer main chain shifts upfield and splits into multiple peaks. Owing to having a lower molecular weight, PAMPP-1 exhibits the characteristic signals of terminal monomeric residues at 13.55, 8.63, 4.66, 3.83, 3.71, and 3.61 ppm, as marked with a cross. However, all of which nearly vanish in the spectrum of higher-molar-mass sample PAMPP-6, suggesting that most of ethynyl and azido groups have been turned into the triazole rings with the increasing polymerization extent. These observations provide further evidence for the conclusion drawn from the IR spectra analysis. Furthermore, it was found that the relative integrated area of both  $a$  and  $a'$  peaks for all polymers is always a unity irrespective of their molecular weights. Apparently, the two peaks are associated with the resonance signals of the triazole methine protons, and the

former is likely from the 1,4-isomeric unit while the latter from the 1,5-isomeric unit.<sup>15</sup> As a result, the fractions of 1,4-substituted triazole ( $F_{1,4}$ ) could be calculated according to their integrals.<sup>16</sup> For all the polymers, the  $F_{1,4}$  values are in the range of 61.9–63.0% (see Table 1), that is, the variation in reaction conditions does not seem to have a large influence on the regioselectivity of the 1,4-triazole linkers.

#### Fluorescence Sensing Ability of PAMPPs to Metal Ions

The binding behavior of PAMPPs toward various metal ions was first examined by means of fluorescence spectroscopy in DMSO. Figure 3 shows the fluorescence change of PAMPP-4 as an example on addition of cations. When excited with the maximum absorption at 310 nm, almost no emission band was observed in the region beyond 350 nm for the free polymer; in other words, the polytriazole is virtually fluorescence silent. However, the addition of zinc ions can significantly provoke its fluorescence emission. In response to this metal ion, the emission intensity around 430 nm increased over 17-fold when 2 equiv of  $\text{Zn}^{2+}$  was added, but other ions tested (i.e.,  $\text{Na}^+$ ,  $\text{K}^+$ ,  $\text{Ag}^+$ ,  $\text{Ca}^{2+}$ ,  $\text{Mg}^{2+}$ ,  $\text{Ni}^{2+}$ ,  $\text{Mn}^{2+}$ ,  $\text{Pb}^{2+}$ ,  $\text{Cd}^{2+}$ ,  $\text{Hg}^{2+}$ ,  $\text{Cu}^{2+}$ ,  $\text{Al}^{3+}$ ,  $\text{Cr}^{3+}$ , and  $\text{Fe}^{3+}$ ) caused no obvious luminescence (Fig. 3).

To gain some insight into the possible interaction patterns between the polymer host and  $\text{Zn}^{2+}$  ion, we designed and synthesized the *N*-salicylidene derivative of (*S*)-1-phenyl-2-(4-butyl-[1,2,3]triazol-1-yl)ethylamine (**6**) as the corresponding

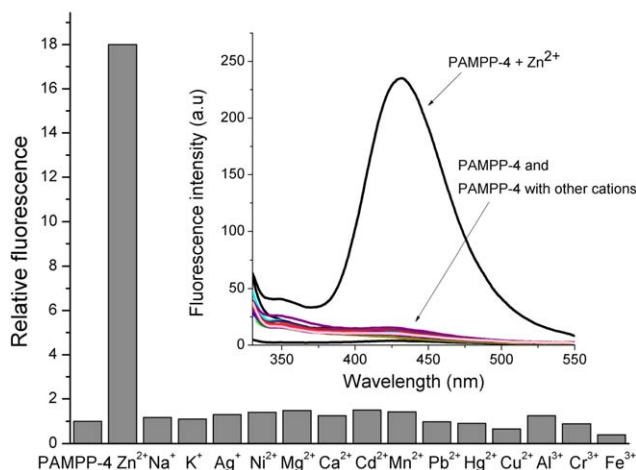


**FIGURE 3** The relative fluorescence intensity of PAMPP-4 (10  $\mu\text{M}$ ,  $\lambda_{\text{ex}} = 310 \text{ nm}$ ) in DMSO in the presence of various metal ions of interest (20  $\mu\text{M}$ ). In the titration,  $\text{Hg}^{2+}$  as mercury perchlorate and other metal ions as their nitrate salts were used. Inset: the corresponding fluorescence spectra of PAMPP-4 in the absence and presence of various metal ions. [Color figure can be viewed in the online issue, which is available at [wileyonlinelibrary.com](http://wileyonlinelibrary.com).]

low molecular weight model compound (Scheme 2 and Supporting Information Fig. S5). The compound is structurally very close to the repeating unit of poly(imine-triazole)s. As expected, the addition of zinc ion to the DMSO solution of **6** also caused a dramatic luminescence enhancement with the emission wavelength shift from 430 to 456 nm ( $\lambda_{\text{ex}} = 320 \text{ nm}$ , Supporting Information Fig. S6). An  $\sim 12$ -fold enhancement in the fluorescence intensity was observed on addition of 2 equiv  $\text{Zn}^{2+}$ , while other cations produced little or no effect. However,  $\text{Zn}^{2+}$  binding of the monomer AMPP leads to an approximately sevenfold increase in the 437 nm emission

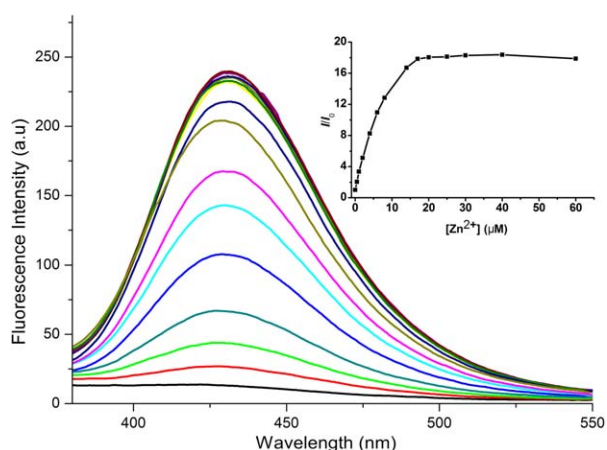


**FIGURE 4** Fluorescence titration profiles of PAMPP-4 (10  $\mu\text{M}$ ) in DMSO with  $\text{Zn}(\text{NO}_3)_2$  (0–6 equiv). Inset shows plots of the relative emission intensity ( $I/I_0$ ) as a function of  $\text{Zn}^{2+}$  concentration (0–60  $\mu\text{M}$ ); the detection limit = 1  $\mu\text{M}$  based on the S/B criteria.  $\lambda_{\text{ex}} = 310 \text{ nm}$ . [Color figure can be viewed in the online issue, which is available at [wileyonlinelibrary.com](http://wileyonlinelibrary.com).]

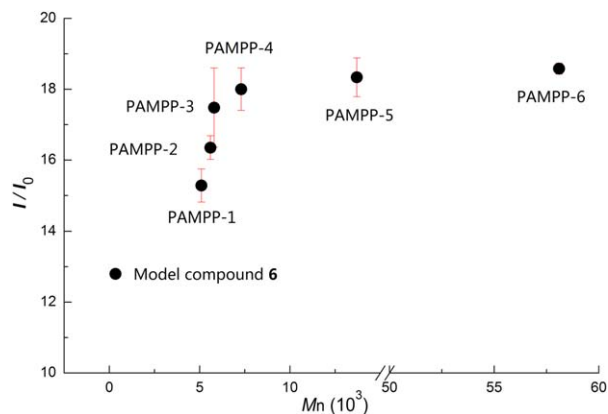


**FIGURE 5** Plot of FE of PAMPPs (10  $\mu\text{M}$ ) in DMSO as a function of  $M_n$  on addition of 2 equiv  $\text{Zn}(\text{NO}_3)_2$ .  $I_0$  is the fluorescence intensity at 430 nm for free polymer, and  $I$  is the fluorescence intensity after adding  $\text{Zn}^{2+}$ ;  $\lambda_{\text{ex}} = 310 \text{ nm}$ . For model compound **6**,  $I/I_0$  represents the FE at 456 nm on addition of 2 equiv  $\text{Zn}(\text{NO}_3)_2$  with an excitation at 320 nm. [Color figure can be viewed in the online issue, which is available at [wileyonlinelibrary.com](http://wileyonlinelibrary.com).]

under the same experimental conditions except for excitation at 310 nm (Supporting Information Figs. S9 and S10). Therefore, the model compound as a  $\text{Zn}^{2+}$  receptor exhibits a higher sensitivity than AMPP in terms of their fluorescence responsiveness, which may be attributed to the fact that the former contains the triazole moiety acting as additional coordination sites for the metal ion.

On the other hand, fluorescence titrations of **6** were also investigated with an excitation at 320 nm (Supporting Information Fig. S7). The peak at 456 nm showed a linear increase with the increase of  $\text{Zn}^{2+}$  ion concentration when the ratio of  $\text{Zn}^{2+}$  and **6** concentrations is below or equal to the ratio of 1:1. When the ratio reached 1:1, however, higher zinc ion concentration did not lead to any further emission enhancement (the

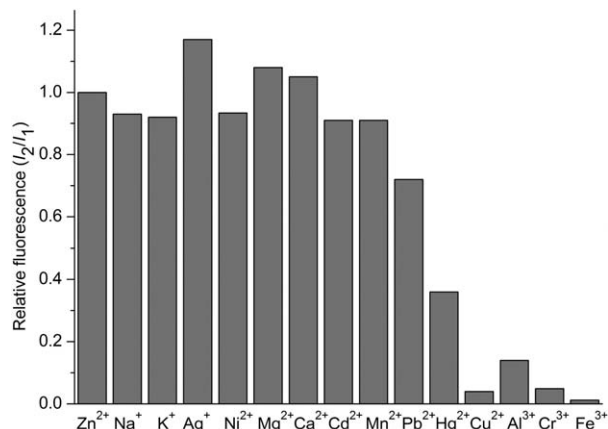


**FIGURE 6** Competitive selectivity of PAMPP-4 (10  $\mu\text{M}$ ) toward  $\text{Zn}^{2+}$  (20  $\mu\text{M}$ ) in the presence of other metal ions (20  $\mu\text{M}$ ) in DMSO solution.  $\text{Hg}^{2+}$  as mercury perchlorate and other various metal ions as their nitrate salts were used in the detection.

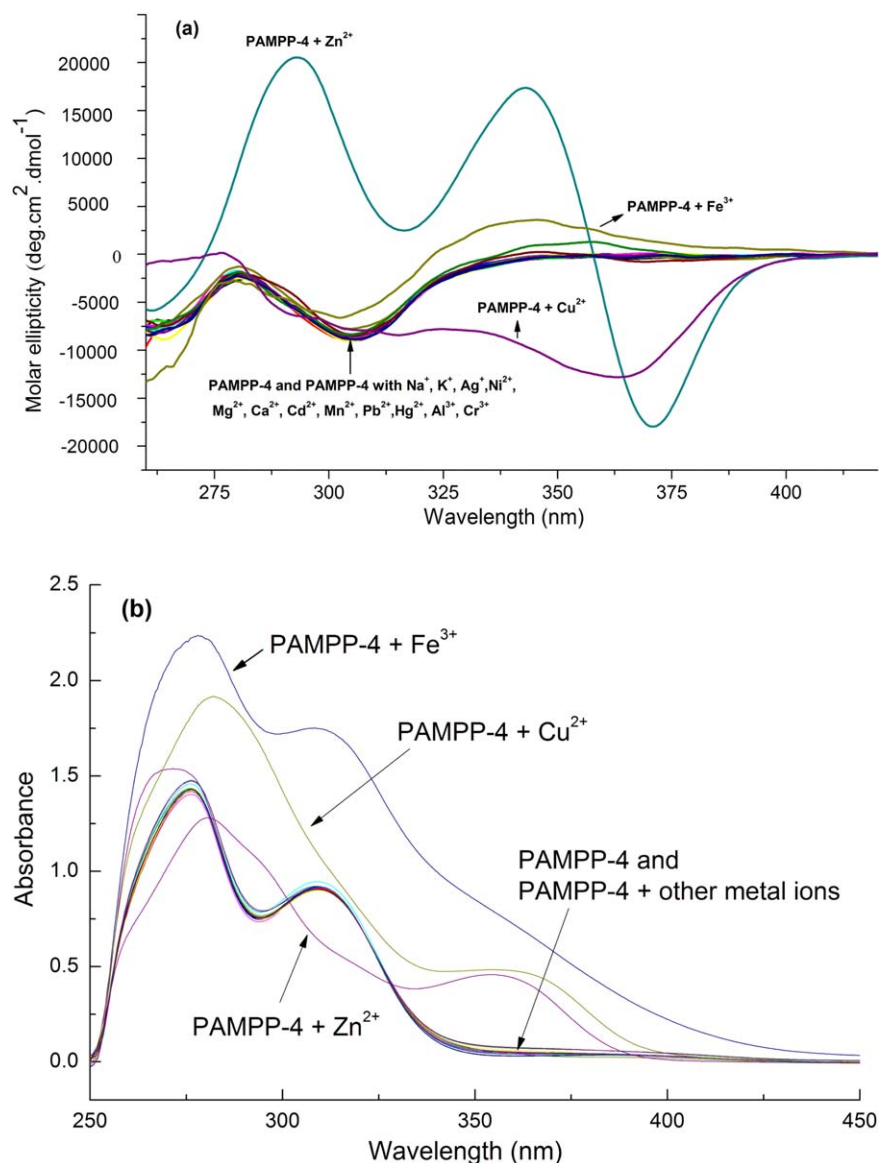


**FIGURE 7** CD (a) and UV-vis (b) responses of PAMPP-4 (100  $\mu\text{M}$ ) to various metal ions (2 equiv.) in DMSO.  $\text{Hg}^{2+}$  as mercury perchlorate and other various metal ions as their nitrate salts were used in the detection. [Color figure can be viewed in the online issue, which is available at [wileyonlinelibrary.com](http://wileyonlinelibrary.com).]

inset of Supporting Information Fig. S7). The binding stoichiometry was supported by the Job's plot of **6** with  $\text{Zn}^{2+}$  (Supporting Information Fig. S8). From the spectral titration data, the association constant ( $K_{\text{ass}}$ ) and the detection limit was determined to be  $8.27 \times 10^4 \text{ M}^{-1}$  and about 5  $\mu\text{M}$ , respectively.

Figure 4 depicts the results of fluorescence titration of PAMPP-4 in DMSO with  $\text{Zn}^{2+}$  under UV irradiation. In the titration experiments using the polymer of 10  $\mu\text{M}$ , the  $\text{Zn}^{2+}$  addition leads to an increase in the 430 nm emission and the increase is saturated with 2 equiv of  $\text{Zn}^{2+}$ . Minimum 1.0  $\mu\text{M}$  concentration of  $\text{Zn}^{2+}$  can be easily detected by a three-fold enhancement in the fluorescence intensity. The detection limit value is lower than or comparable to those observed

with many fluorescent  $\text{Zn}^{2+}$  sensors.<sup>10,14,17</sup> Interestingly, the magnitude of fluorescence enhancements (FE) is positively correlated with the polymer molar masses in the range  $5.1 \times 10^3 \text{ g mol}^{-1} < M_n < 7.3 \times 10^3 \text{ g mol}^{-1}$ , as seen in Figure 5. On addition of  $\text{Zn}^{2+}$  (2 equiv) the FE value for PAMPP-4 ( $M_n = 7.3 \times 10^3$ ) is roughly 1.2 and 1.6 times as great as for PAMPP-1 ( $M_n = 5.1 \times 10^3$ ) and the model compound **6**, respectively. However, a further increase in the molar mass does not significantly affect the fluorescence responsiveness. The comparison of the detection limits of **6** and of PAMPP-4 (5.0  $\mu\text{M}$  vs. 1.0  $\mu\text{M}$ ; also see Fig. 4 and Supporting Information Fig. S7 inset) in combination with the observed  $M_n$  – FE relationship demonstrates that these poly(imine-triazole)s are more effective as a fluorescent sensor for selective  $\text{Zn}^{2+}$  recognition compared to its small molecule counterparts,

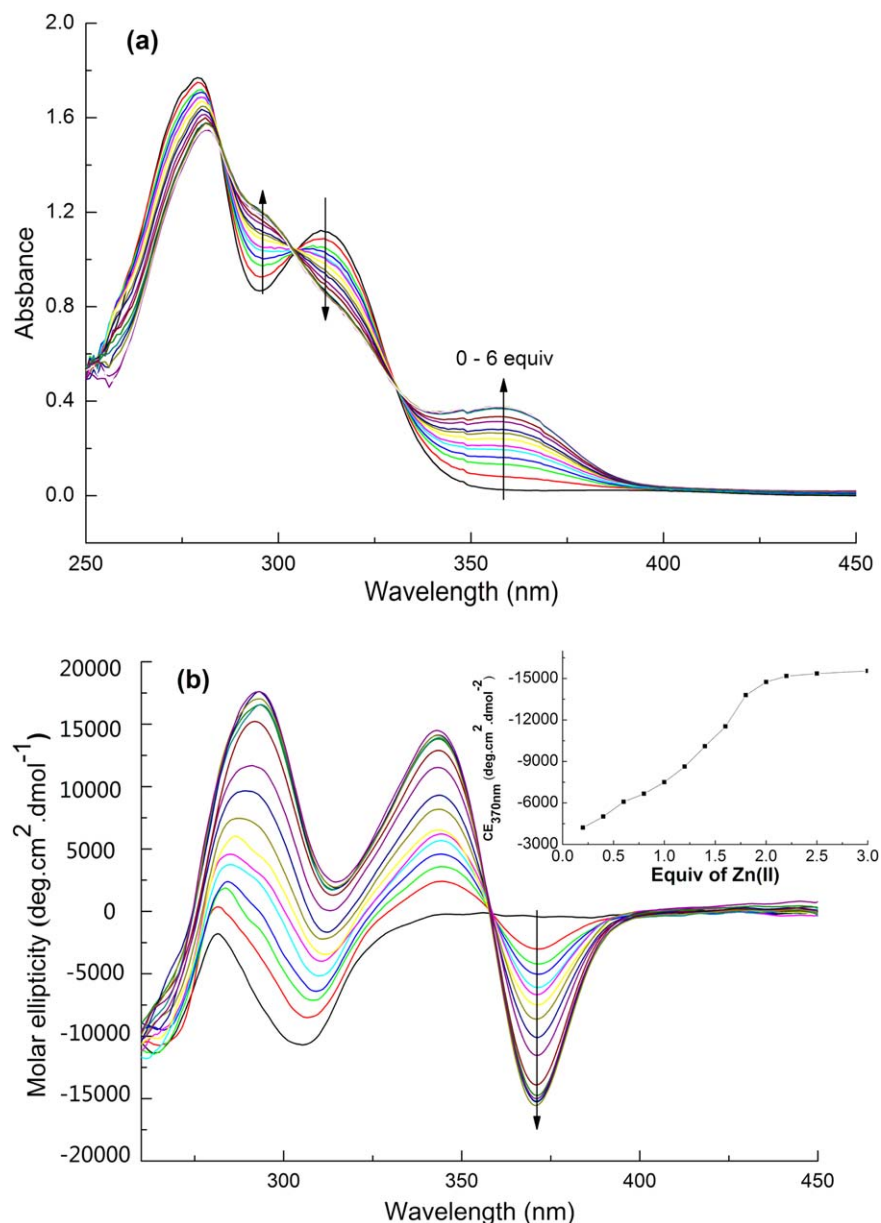


**FIGURE 8** UV-vis (a) and CD (b) titration profiles of PAMPP-4 (100  $\mu\text{M}$ ) with  $\text{Zn}(\text{NO}_3)_2$  (0–3 equiv) in DMSO. Inset displays plots of the CE intensity at 370 nm as a function of  $\text{Zn}^{2+}$  concentration (0–3 equiv). [Color figure can be viewed in the online issue, which is available at [wileyonlinelibrary.com](http://wileyonlinelibrary.com).]

which could be explained by the cooperative effects of chromophores connected to the polymer main chain.<sup>11,12</sup>

As inferred from the competitive experiments (Fig. 6), the poly(imine-triazole) sensor exhibited a strong preference for  $\text{Zn}^{2+}$  over other metal cations including  $\text{Cd}^{2+}$  as in the case of the previously reported Schiff base receptor.<sup>10</sup> It is noteworthy that such a chemosensor capable of distinguishing between  $\text{Zn}^{2+}$  and  $\text{Cd}^{2+}$  is highly desirable, because recognition of the two metal ions with similar chemical properties is still challenging.<sup>18</sup> Addition of  $\text{Ag}^+$ ,  $\text{Mg}^{2+}$ , or  $\text{Ca}^{2+}$  promoted a small increase of the  $\text{Zn}^{2+}$ -induced luminescence, whereas the presence of  $\text{Pb}^{2+}$ ,  $\text{Hg}^{2+}$ , and  $\text{Al}^{3+}$

caused fluorescence quenching of ca. 30, 60, and 85%, respectively. The metal cations including  $\text{Cu}^{2+}$ ,  $\text{Cr}^{3+}$ , and  $\text{Fe}^{3+}$  severely interfered the detection of  $\text{Zn}^{2+}$  probably due to the competing complexation of imine-triazole moieties with these metals. In general, these transition metal ions are considered as fluorescence quenchers, like other heavy metals with partially filled d-shells.<sup>14,19</sup>

#### CD and UV-vis Response Behavior of PAMPPs Toward Metal Ions

Chiral polymers would adopt different asymmetric conformations or aggregates on complexation with possible target



species. Therefore, one attractive feature of chiral chemosensors is their capacity of translating a recognition event into the chiroptical signal. As an example, the CD and UV-vis spectra of PAMPP-4 as well as its specific rotation were measured in the absence and presence of metal ions in DMSO. As shown in Figure 7, the free polymer presented a noticeable CD signal at 250–450 nm that exhibits a single negative CE around 306 nm. The two bands of the UV-vis spectrum in this region are assignable to the triazole and salicylidene chromophores of the polymer backbone. After the addition of  $\text{Zn}^{2+}$  (2 equiv), a sharp spectral change was observed for the polymer solution, wherein the 306-nm CE disappeared while one negative and two positive CEs emerged at 370, 343, and 288 nm, respectively. On the contrary, other cations tested including  $\text{Na}^+$ ,  $\text{K}^+$ ,  $\text{Ag}^+$ ,  $\text{Pb}^{2+}$ ,  $\text{Cd}^{2+}$ ,  $\text{Mg}^{2+}$ ,  $\text{Ca}^{2+}$ ,  $\text{Ni}^{2+}$ ,  $\text{Mn}^{2+}$ ,  $\text{Al}^{3+}$ ,  $\text{Cr}^{3+}$ , and  $\text{Fe}^{3+}$  did not induce any noticeable variation in the CD profile of the chiral polymer. Although the addition of  $\text{Cu}^{2+}$  disturbed the polymer's CD pattern, the spectral changes induced by this ion are totally different from that found in the case of  $\text{Zn}^{2+}$ . In this way, the selective CD responses exhibited by the polymer sensor allowed for the discrimination of  $\text{Zn}^{2+}$  from  $\text{Al}^{3+}$ ,  $\text{Cu}^{2+}$ ,  $\text{Cr}^{3+}$ , and  $\text{Fe}^{3+}$  ions that would produce serious interference in the fluorescence detection. The fact that PAMPP-4 give rise to a strong induced CD signal suggests the formation of a Zn(II)-containing polymer complex with an ordered structure, but it does not seem to exist in a helical conformation as judged from the small  $[\alpha]_D^{20}$  change (e.g., from +8.7 to +37.1 for PAMPP-4 on  $\text{Zn}^{2+}$  binding).

Figure 8 plots the changes in the absorption and CD spectra of PAMPP-4 in DMSO in the presence of different concentration of  $\text{Zn}^{2+}$  cations. During the course of the titration, a significant decrease in the band at 310 nm and the emergence of a new band centered at 358 nm were observed with two clear isosbestic points at 330 and 304 nm, respectively [Fig. 8(a)]. Correspondingly, the polymer bound  $\text{Zn}^{2+}$  ion gave typical exciton-coupled CD spectra [Fig. 8(b)]. Such an induced CD couplet should arise from the enhanced interaction between nearby chromophores embedded in a chiral environment owing to the host–guest complexation. Also, the amplitude of the induced CEs is linearly dependent on the  $\text{Zn}^{2+}$  concentration (20–200  $\mu\text{M}$ ), as can be seen in Figure 8(b) inset, which would allow the quantitative determination in a broader concentration range.

We also examined the relative intensities of the CD-signals observed for the poly(imine-triazole)s having different molar masses. The results showed that there was no obvious  $M_n$  dependence of the 306-nm CE intensity [Supporting Information Fig. S11(a)]. Moreover, the  $\text{Zn}^{2+}$ -induced CD responses ( $\text{CE}_{370\text{ nm}}$ ) were not greatly affected by the polymer molar masses except for the samples of  $M_n$  lower than  $\sim 7 \times 10^3$  [Supporting Information Fig. S11(b)], in contrast to the evident  $M_n$  dependence of fluorescent enhancement (see Fig. 5). However, it should be noted that only slight spectral responses can be detected for model compound **6** or AMPP, even when 150 equivalents of  $\text{Zn}^{2+}$  were added (Supporting

Information Fig. S12), indicating that the chiral polymers as a sole  $\text{Zn}^{2+}$  probe offer distinctive advantages over these small molecule analogs.

## CONCLUSIONS

In summary, we designed a AB type of clickable monomer (*S*)-2-[(2-azido-1-phenylethylimino)methyl]-5-propargyloxyphenol (AMPP) and conducted the metal-free click polymerization to synthesize the corresponding poly(imine-triazole)s. By using a stepwise heating-up process, the thermally induced polyaddition produced the desired main-chain chiral polymers with controlled molar masses ( $M_n = 5.1 \times 10^3 - 58.1 \times 10^3$ ) and narrower polydispersity (PDI = 1.38 - 1.68). It was demonstrated that these chiral polytriazoles can be employed as a novel sensor for dual-mode fluorescent and CD detection of zinc ions in DMSO. The polymer probe displays a moderate fluorescent selectivity for  $\text{Zn}^{2+}$  with a large turn-on emission. Although the metal cations including  $\text{Al}^{3+}$ ,  $\text{Cu}^{2+}$ ,  $\text{Cr}^{3+}$ , and  $\text{Fe}^{3+}$  would interfere the detection of  $\text{Zn}^{2+}$  due to their fluorescence quenching, discrimination of  $\text{Zn}^{2+}$  from these metal ions can be facily achieved by the chiral sensor because the  $\text{Zn}^{2+}$ -induced CD spectral change is not only noticeable but also significantly different from those with other ions tested.

## ACKNOWLEDGMENT

We gratefully acknowledge the support from the Natural Science Foundation of China (Grant No. 21074107).

## REFERENCES AND NOTES

- 1 H. C. Kolb, M. Finn, K. B. Sharpless, *Angew. Chem. Int. Ed.* **2001**, *40*, 2004–2021.
- 2 R. K. Iha, K. L. Wooley, A. M. Nyström, D. J. Burke, M. J. Kade, C. Hawker, *Chem. Rev.* **2009**, *109*, 5620–5686.
- 3 (a) V. V. Rostovtsev, L. G. Green, V. V. Fokin, K. B. Sharpless, *Angew. Chem. Int. Ed.* **2002**, *41*, 2596–2599; (b) M. Meldal, C. W. Tornøe, *Chem. Rev.* **2008**, *108*, 2952–3015.
- 4 (a) D. Fournier, R. Hoogenboom, U. S. Schubert, *Chem. Soc. Rev.* **2007**, *36*, 1369–1380; (b) A. Qin, J. W. Lam, B. Z. Tang, *Macromolecules* **2010**, *43*, 8693–8702; (c) W. H. Binder, R. Sachsenhofer, *Macromol. Rapid Commun.* **2008**, *29*, 952–981; (d) P. L. Golas, K. Matyjaszewski, *Chem. Soc. Rev.* **2010**, *39*, 1338–1354; (e) M. Juriček, P. H. Kouwer, A. E. Rowan, *Chem. Commun.* **2011**, *47*, 8740–8749; (f) I. A. Miladi, B. P. Mudraboyina, A. Oueslati, E. Drockenmuller, H. B. Romdhane, *J. Polym. Sci. Part A: Polym. Chem.* **2014**, *52*, 223–231; (g) Q. Wang, H. Li, Q. Wei, J. Z. Sun, J. Wang, X. A. Zhang, A. Qin, B. Z. Tang, *Polym. Chem.* **2013**, *4*, 1396–1401; (h) J. Han, D. Zhu, C. Gao, *Polym. Chem.* **2013**, *4*, 542–549; (i) H. He, C. Gao, *Curr. Org. Chem.* **2011**, *15*, 3667–3691; (j) J. Han, B. Zhao, Y. Gao, A. Tang, C. Gao, *Polym. Chem.* **2011**, *2*, 2175–2178; (k) J. Han, C. Gao, *Nano-Micro Lett.* **2010**, *2*, 213–226; (l) A. Qin, J. W. Lam, B. Z. Tang, *Chem. Soc. Rev.* **2010**, *39*, 2522–2544. (m) H. Li, J. Sun, A. Qin, B. Z. Tang, *Chin. J. Polym. Sci.* **2012**, *30*, 1–15.
- 5 (a) Y. Hua, A. H. Flood, *Chem. Soc. Rev.* **2010**, *39*, 1262–1271; (b) H. F. Chow, K. N. Lau, Z. Ke, Y. Liang, C. M. Lo, *Chem. Commun.* **2010**, *46*, 3437–3453; (c) A. C. Fahrenbach, J. F. Stoddart, *Chem. Asian J.* **2011**, *6*, 2660–2669.

- 6** (a) Z. Chen, D. R. Dreyer, Z. Q. Wu, K. M. Wiggins, Z. Jiang, C. W. Bielawski, *J. Polym. Sci. Part A: Polym. Chem.* **2011**, *49*, 1421–1426; (b) X. M. Liu, L. D. Quan, J. Tian, F. C. Laquer, P. Ciborowski, D. Wang, *Biomacromolecules* **2010**, *11*, 2621–2628; (c) Y. Wang, R. Zhang, N. Xu, F. S. Du, Y. L. Wang, Y. X. Tan, S. P. Ji, D. H. Liang, Z. C. Li, *Biomacromolecules* **2011**, *12*, 66–74; (d) J. Guo, Y. Wei, D. Zhou, P. Cai, X. Jing, X. S. Chen, Y. Huang, *Biomacromolecules* **2011**, *12*, 737–746; (e) A. M. Eissa, E. Khosravi, *Eur. Polym. J.* **2011**, *47*, 61–69.
- 7** K. Itomi, S. Kobayashi, K. Morino, H. Iida, E. Yashima, *Polym. J.* **2009**, *41*, 108–109.
- 8** (a) X. Huang, Y. Dong, J. Meng, Y. Cheng, C. Zhu, *Synlett* **2010**, 1841–1844; (b) X. Huang, J. Meng, Y. Dong, Y. Cheng, C. Zhu, *Polymer* **2010**, *51*, 3064–3067.
- 9** (a) A. Qin, J. W. Lam, L. Tang, C. K. Jim, H. Zhao, J. Sun, B. Z. Tang, *Macromolecules* **2009**, *42*, 1421–1424; (b) Q. Wang, M. Chen, B. Yao, J. Wang, J. Mei, J. Z. Sun, A. Qin, B. Z. Tang, *Macromol. Rapid Commun.* **2013**, *34*, 796–802; (c) H. Li, H. Wu, E. Zhao, J. Li, J. Sun, A. Qin, B. Z. Tang, *Macromolecules* **2013**, *46*, 3907–3914.
- 10** M. Zhang, W. Lu, J. Zhou, G. Du, L. Jiang, J. Ling, Z. Shen, *Tetrahedron* **2014**, *70*, 1011–1015.
- 11** (a) H. N. Kim, Z. Guo, W. Zhu, J. Yoon, H. Tian, *Chem. Soc. Rev.* **2011**, *40*, 79–93; (b) G. He, N. Yan, H. Kong, S. Yin, L. Ding, S. Qu, Y. Fang, *Macromolecules* **2011**, *44*, 703–710; (c) Y. Tian, B. R. Shumway, D. R. Meldrum, *Chem. Mater.* **2010**, *22*, 2069–2078.
- 12** (a) D. Chen, W. Lu, G. Du, L. Jiang, J. Ling, Z. Shen, *J. Polym. Sci. Part A: Polym. Chem.* **2012**, *50*, 4191–4197; (b) B. Liu, W. Lu, G. Du, D. Chen, J. Ling, L. Jiang, Z. Shen, *Acta Polym. Sin.* **2013**, 436–442; (c) W. Lu, J. Zhou, K. Liu, D. Chen, L. Jiang, Z. Shen, *J. Mater. Chem. B* **2013**, *1*, 5014–5020.
- 13** In the control experiments, the click polymerization of AMPP was carried out in DMF in the present of CuI/Et<sub>3</sub>N. The reaction mixture was stirred magnetically at 50°C for 24 h, diluted with DMF, and passed through neutral alumina to remove the copper catalyst from the resultant products. However, the complete elimination of metal residual was not achieved even if dialysis method was finally employed for the purification judging from the color Cu(II) species.
- 14** (a) S. C. Burdette, S. J. Lippard, *Inorg. Chem.* **2002**, *41*, 6816–6823; (b) Z. Xu, K. H. Baek, H. N. Kim, J. Cui, X. Qian, D. R. Spring, I. Shin, J. Yoon, *J. Am. Chem. Soc.* **2010**, *132*, 601–610.
- 15** Usually, the resonance signals of 1,4-isomeric triazole CH protons appear at a downfield compared to the corresponding CH of 1,5-isomeric units. See: ref. 9.
- 16** Fraction of 1,4-disubstituted 1,2,3-triazoles are calculated according to the formula  $F_{1,4} = I_a / (I_a + I_a')$ , where  $I_a$  and  $I_a'$  represent the integral of the signals at 8.11 and 7.73 ppm, respectively.
- 17** (a) S. A. Silva, A. Zavaleta, D. E. Baron, O. Allam, E. V. Isidor, N. Kashimura, J. M. Percarpio, *Tetrahedron Lett.* **1997**, *38*, 2237–2240; (b) Z. Xu, G. Kim, S. Han, M. Jou, C. Lee, I. Shin, J. Yoon, *Tetrahedron* **2009**, *65*, 2307–2312; (c) M. M. Henary, Y. Wu, C. J. Fahrni, *Chem. Eur. J.* **2004**, *10*, 3015–3025; (d) L. Jiang, L. Wang, M. Guo, G. Yin, R. Y. Wang, *Sens. Actuators B* **2011**, *156*, 825–831; (e) Z. Q. Guo, G. H. Kim, I. Shin, J. Yoon, *Biomaterials* **2012**, *33*, 7818–7827; (f) X. Ni, X. Zeng, C. Redshaw, T. Yamato, *J. Org. Chem.* **2011**, *76*, 5696–5702; (g) V. Bhalla, R. Tejpal, M. Kumar, *Dalton Trans.* **2012**, *41*, 10182–10188.
- 18** (a) H. Y. Lin, P. Y. Cheng, C. F. Wan, A. T. Wu, *Analyst* **2012**, *137*, 4415–4417; (b) K. Hanaoka, K. Kikuchi, H. Kojima, Y. Urano, T. Nagano, *J. Am. Chem. Soc.* **2004**, *126*, 12470–12476; (c) S. C. Burdette, C. J. Frederickson, W. Bu, S. J. Lippard, *J. Am. Chem. Soc.* **2003**, *125*, 1778–1779; (d) J. Du, J. Fan, X. Peng, H. Li, S. Sun, *Sens. Actuators B* **2010**, *144*, 337–341.
- 19** R. T. Bronson, M. Montalti, L. Prodi, N. Zaccheroni, R. D. Lamb, N. K. Dalley, R. M. Izatt, J. S. Bradshaw, P. B. Savage, *Tetrahedron* **2004**, *60*, 11139–11144.